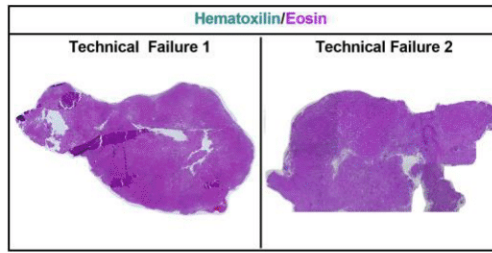
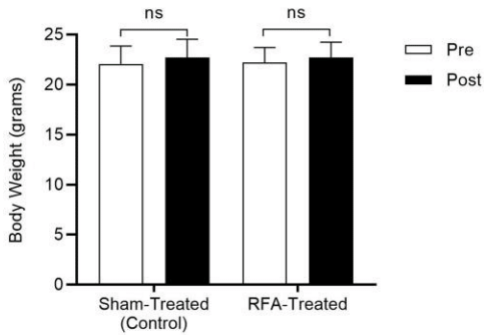
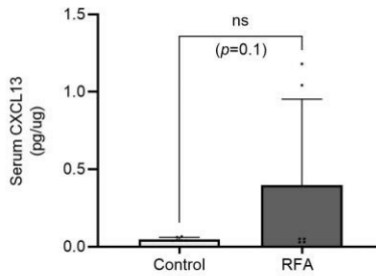
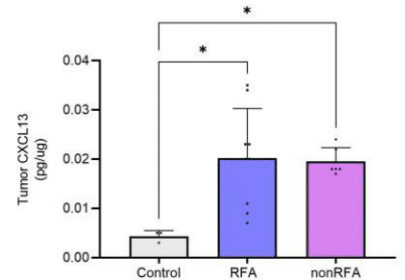
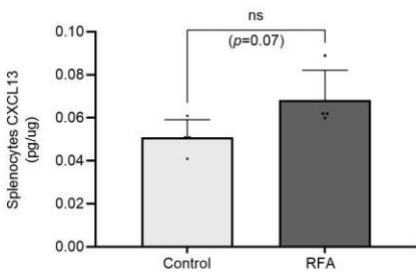
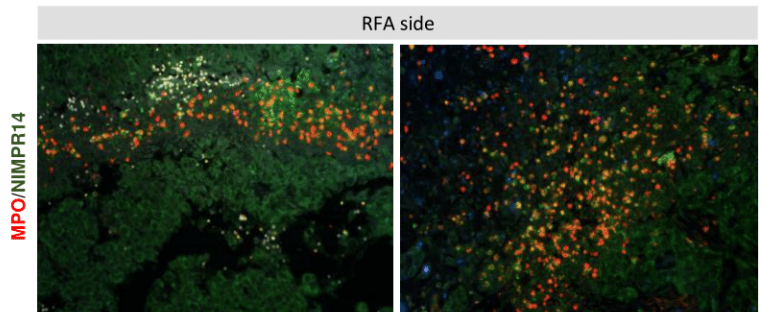
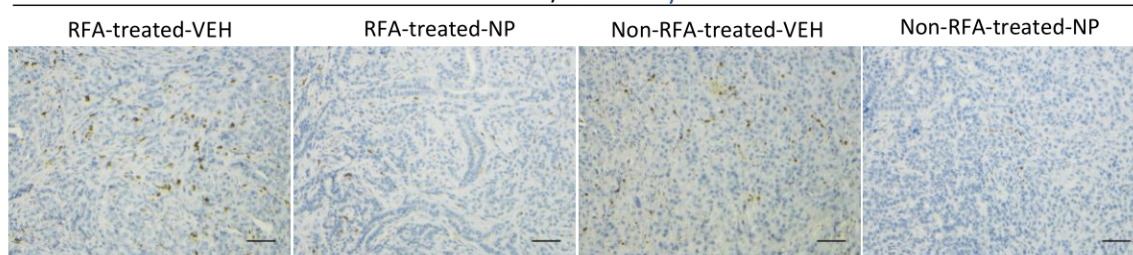
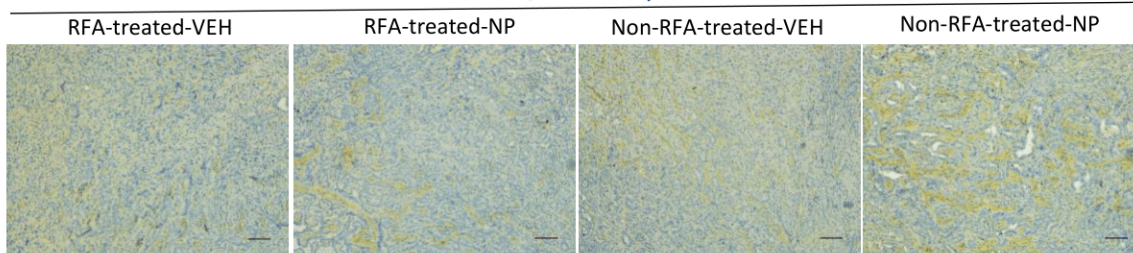
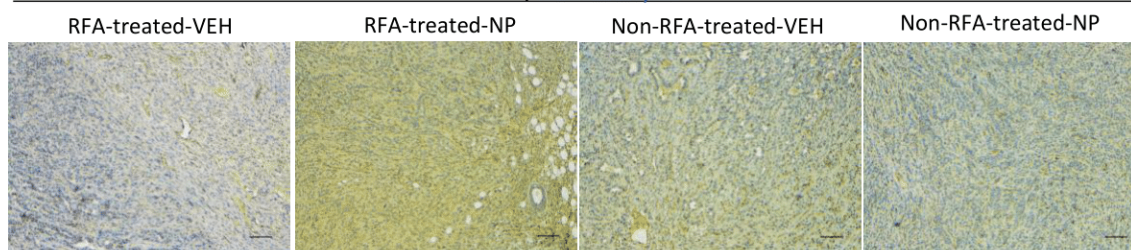


A

Experiment Summary					
Control mice (n): 8; Treated mice (n): 10					
RFA - Technical success					
Successful	n = 8	80%	Not successful	n = 2	20%
RFA - Response (local and abscopal)					
RFA-side	n	(%)	non-RFA side	n	(%)
Responsive	8	100	Responsive	7	87.5
Non-Responsive	0	--	Non-Responsive	1	12.5

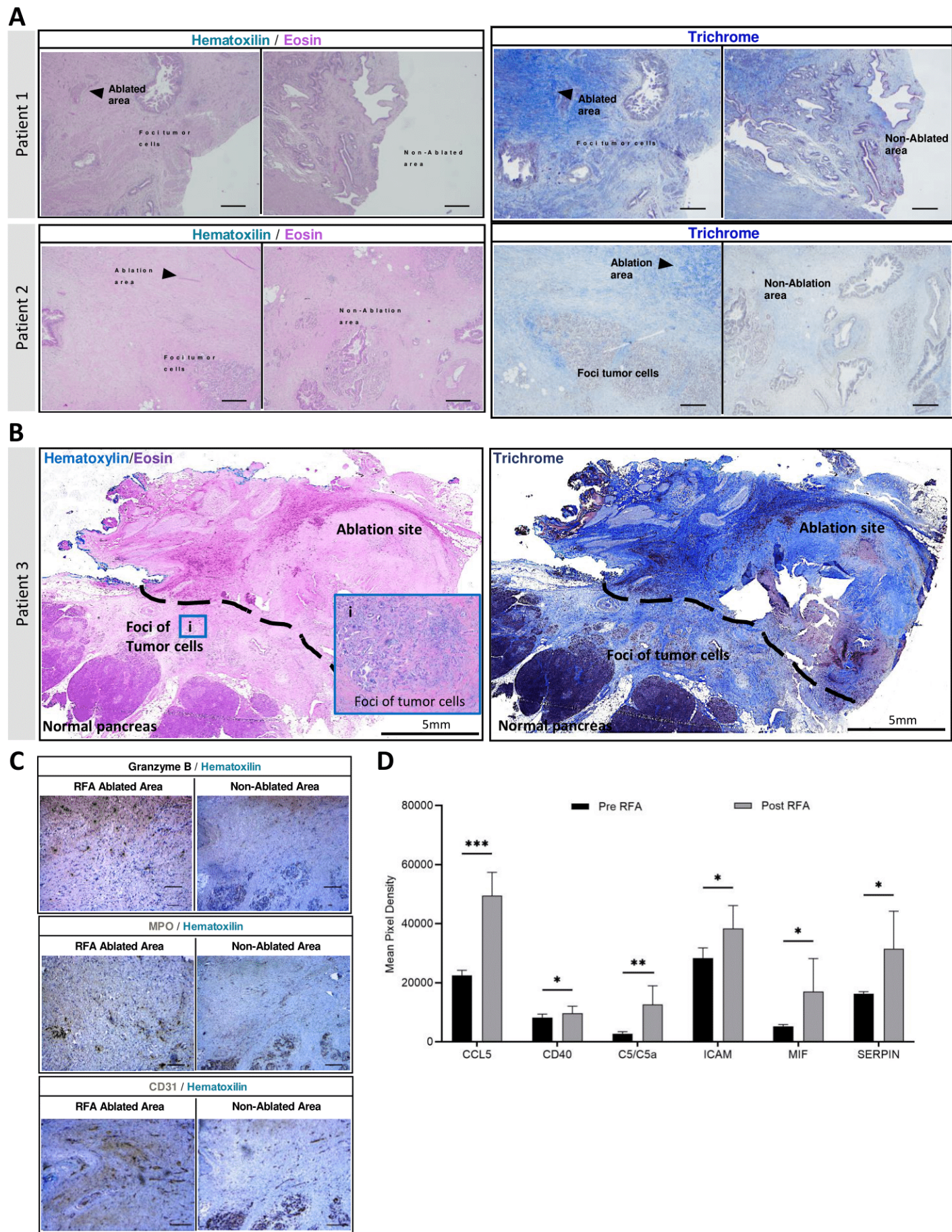
B**C****D****E****F****G**

Supplementary Figure 1. A, Experiment summary. A total of 8 mice were Sham-treated and classified as control group. Another 10 mice were ablated in one flank and technique effectiveness in RFA-treated tumors was analyzed by necrotic core assessment, considering the presence of necrotic cores as positive sign for ablation success. 8 out of 10 (80%) treated mice showed necrotic cores. Mice with successful RFA technique were considered for further studies. In these mice the abscopal effect was observed in 87.5% of cases. Ablation technique was not successful in 2 out of 10 mice (20%), as assessed by the absence of necrotic cores in RFA-treated tumors. Unsuccessful RFA technique mice were not considered for further analysis. **B**, H&E composite staining of RFA technical failure indicating no evident necrosis in tumor cores. RFA technical failure mice were excluded from analysis. **C**, RFA treatment did not affect body weight in Sham-treated control nor in RFA-treated mice. **D-F**, CXCL13 levels were analyzed by ELISA. Serum (**D**), tumor (**E**) and splenocytes (**F**) levels were increased in RFA treated mice when compared to Sham treated controls. **G**, IF staining indicate significant overlap between MPO and NIMPR14 in RFA-treated tumors. *, $P \leq 0.05$; n.s., not significant.

ANIMPR14/**Hematoxylin****B**aSMA/**Hematoxylin****C**CD31/**Hematoxylin**

Supplementary Figure 2. A, Depletion of Ly6G+ cells was confirmed by IHC staining ($n = 3$ per group). **B**, Representative aSMA IHC staining ($n = 3$ per group). **C**, Representative IHC staining for CD31+ cells ($n = 3$ per group). Scale bars are 50uM.

Supplementary Figure 3



Supplementary Figure 3. RFA tumor microenvironment and immune modulation in human pancreatic tumors. **A**, H&E (**left**) and trichrome (**right**) staining of higher magnification RFA-ablated and non-ablated areas from two Stage I resected tumors from PDAC patients treated with chemotherapy in combination with EUS-RFA. Necrosis and collagen deposition are pronounced in the RFA ablated areas compared to non-ablated regions in all samples as previously observed in the RFA preclinical mouse model. **B**, Composite H&E (**left**) and trichrome (**right**) staining of a Stage III locally advanced human pancreatic cancer resected tumor showing both RFA-ablated and non-ablated areas, with evident necrosis in ablated site, a Foci of tumor cells (**i**) and residual normal pancreatic tissue. Strong collagen deposition was also observed in the resected tumors in ablation site. **C**, Similar to our findings in the RFA preclinical mouse model, Granzyme B (**top**), MPO (**middle**) and CD31+ (**bottom**) are induced after RFA treatment in human pancreatic cancer in both RFA-ablated (**left**) and non-ablated (**right**) areas, as shown by immunohistochemistry staining. **D**, CCL5, CD40, C5/C5a, CXCL12, ICAM, MIF and SERPIN were elevated in serum from a PDAC patient Post ablation when compared to Pre-ablation measurements. Scale bars are 50uM. Multiple t test was used for serum proteome analysis. *, $P \leq 0.05$; **, $P \leq 0.01$; ***, $P \leq 0.001$.